JACS
JOURNAL OF THE AMERICAN CHEMICAL SOCIETY
Article
pubs.acs.org/JACS

Aromatic Side Chain Water-to-Lipid Transfer Free Energies Show a Depth Dependence across the Membrane Normal

Sarah K. McDonald and Karen G. Fleming*

T.C. Jenkins Department of Biophysics, Johns Hopkins University, Baltimore, Maryland 21218, United States

Supporting Information

ABSTRACT: Quantitating and understanding the physical forces responsible for the interactions of biomolecules are fundamental to the biological sciences. This is especially challenging for membrane proteins because they are embedded within cellular bilayers that provide a unique medium in which hydrophobic sequences must fold. Knowledge of the energetics of protein−lipid interactions is thus vital to understand cellular processes involving membrane proteins. Here we used a host−guest mutational strategy to calculate the Gibbs free energy changes of water-to-lipid transfer for the aromatic side chains Trp, Tyr, and Phe as a function of depth in the membrane. This work reveals an energetic gradient in the transfer free energies for Trp and Tyr, where transfer was most favorable to the membrane interfacial region and comparatively less favorable into the bilayer center. The transfer energetics follows the concentration gradient of polar atoms across the bilayer normal that naturally occurs in biological membranes. Additional measurements revealed nearest-neighbor coupling in the data set are influenced by a network of aromatic side chains in the host protein. Taken together, these results show that aromatic side chains contribute significantly to membrane protein stability through either aromatic−aromatic interactions or placement at the membrane interface.

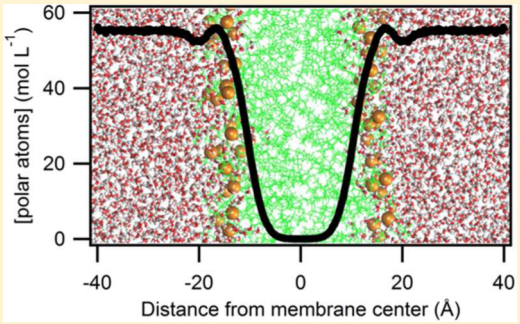

INTRODUCTION

Membranes are physical barriers of the cell that enclose and protect cellular processes. Proteins that fold into the membrane are important for sensing and reacting to biological signals in the extracellular environment. Some ways that membrane proteins respond to such stimuli are through ligand binding, allostery, or conformational change. Because a significant amount of membrane protein surface area is embedded within the bilayer, the magnitudes of membrane protein−lipid interactions are essential to interrogate the stabilities and structures of these biologically relevant states. Moreover, because membrane proteins constitute about 60% of drug targets,[1] a complete understanding of membrane protein interactions is vital for interpreting disease-causing mutations and will aid in the design and improvement of drugs.

The chemistry of side chains defines membrane protein structures within lipid bilayers. For example, consider the hydrophobic effect in protein folding, where the exclusion of nonpolar side chains by water is a large entropic driving force for the unfolded-to-folded transition.[2] For soluble proteins, hydrophobic collapse shapes the native structure by largely burying nonpolar side chains in the interior while leaving polar/charged groups facing bulk water.[3] Similarly, nonpolar side chains in membrane proteins are enriched on the folded protein surface, where they are exposed to the phospholipid solvent.[4]

In addition, the first membrane protein crystal structures revealed a striking pattern in the spatial positioning of lipid-facing Trp and Tyr side chains along the bilayer normal.[5] This observation was confirmed by Wallin et al.[6] with an analysis of side chain distributions in cytochrome *c* oxidase. This analysis has since been extended through independent studies by Ulmschneider et al.[7] and Senes et al.[8] with large sets of α-helical crystal structures, which showed the statistical enrichment of Trp and Tyr at the interfacial region. In addition to Trp and Tyr, Phe also shows a similar enrichment in β-barrel structures, as demonstrated by Hsieh et al.[9] and Slusky and Dunbrack.[10] These side chains form an aromatic "belt" around the protein located at the water−hydrocarbon interface that has been proposed to "anchor" membrane protein structure to the bilayer.[11]

Trp and Tyr are composed of an aromatic ring and contain polar atoms that are traditional hydrogen-bond donors. Jacobs and White[12] showed that Trp pentapeptides partition into the interfacial region of 1,2-dioleoyl-*sn*-glycero-3-phosphocholine (DOPC) membranes. These authors noted that the amphiphilic character of the Trp side chains is important for interfacial localization because this region provides a complementary chemical environment. Correspondingly, Wimley and White[13] showed that Trp, Tyr, and Phe partition with favorable free energies in water-to-interface measurements with a rank order of Trp > Phe > Tyr. However, traditional hydrogen bonding may be less important than previously thought. An NMR study by Yau et al.[14] reporting on the location of Trp

Received: April 4, 2016
Published: June 2, 2016

DOI: 10.1021/jacs.6b03460
J. Am. Chem. Soc. 2016, 138, 7946−7950

analogues (including indene, which lacks hydrogen-bond donors) in a 1-palmitoyl-2-oleoyl-*sn*-glycero-3-phosphocholine (POPC) membrane showed that all of these analogues partitioned near the glycerol region. This suggests that the preference for this area of the membrane is not dependent on hydrogen bonding alone. Instead, the authors concluded that the large, flat shape of Trp may be responsible for exclusion from the hydrophobic core because entropically this packing would be unfavorable.

Experimental studies with model systems have attempted to address this question of energetics in membranes. As Wolfenden recently reviewed, a simple conclusion is not straightforward because the chemical nature of nonpolar solvents and the solubility of water within them can change the rank order of water-to-solvent transfer free energies.[15] Moreover, it is well-established that the water concentration in a membrane is not constant. As shown by Wiener, Wimley, and White, the biological membrane naturally possesses a gradient of polarity due largely to a changing water density across the bilayer.[16,17] MacCallum, Bennett, and Tieleman[18] described this steep concentration gradient as occurring on a nanometer length scale. Overall, it is clear that this property of the lipid bilayer represents a sharply changing chemical environment for side chain−lipid interactions. From a physical chemistry viewpoint, the energetic contributions of side chains to membrane protein folding should reflect this changing environment within an actual membrane.

In this work, we measured the water-to-lipid transfer free energies for the Trp, Tyr, and Phe side chains as a function of depth across the bilayer normal. As opposed to nonpolar solvents, our experiments used actual lipid bilayers containing the polarity gradient found in biological membranes. Such bilayers are also well-described by molecular dynamics (MD) simulations, which provide atomistic views of the structure that may inform on the energetics. We found that Trp and Tyr thermodynamically prefer the membrane interface, which is more hydrated than the membrane center. The energy data were well-modeled using the concentration of polar atoms present at host sites calculated from a neat 1,2-didodecanoyl-*sn*-glycero-3-phosphocholine (DLPC) MD simulation. Our results are the first to show experimentally that aromatic side chains favorably contribute to membrane protein stability in a membrane-depth-dependent manner in which partitioning to the interface is favored over burial in the center.

RESULTS

Aromatic Side Chain Energies Are Most Favorable at the Membrane Interface. Figure 1A shows the host sites for mutagenesis in outer membrane phospholipase A (OmpLA) (native to *Escherichia coli*; all variants are shown in Table S1). Figure 1B shows the thermodynamic cycle used to calculate the Gibbs free energy of water-to-lipid transfer relative to alanine mutations. We verified that all of the variants fold reversibly and are enzymatically active when folded (Figures S1 and S2).

Folding titrations using chemical denaturation were fit (Figure S3) to determine the folding free energies of all variants (Table S2), and $\Delta\Delta G^{\circ}_{W,L}$ values (Table S3) were calculated according to the equation shown in Figure 1B. For variants 173Y and 173W, the transfer free energies were determined with a reference state where Y195 was mutated to Ala (e.g., 173A/195A). We gained a data point in the Trp and Tyr data from our double-variant cycle analysis with site 195 presented in the next section.

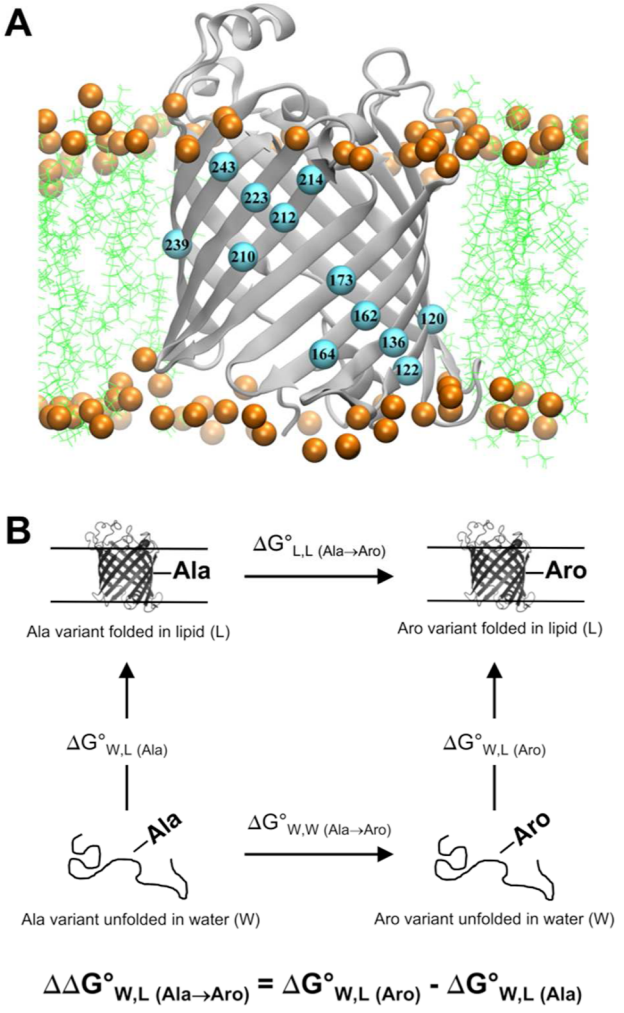

Figure 1. Thermodynamic cycle illustrating how water-to-lipid side chain energies are calculated. (A) Snapshot from an MD simulation of OmpLA (Protein Data Bank entry 1qd5)[19] embedded in a DLPC membrane. Lipid tails are shown as green lines and phosphorus atoms as gold spheres. Highlighted in cyan are the Cα atoms of host sites with residue numbers indicated. This image was created using visual molecular dynamics (VMD).[20] (B) Thermodynamic cycle used to determine side chain water-to-lipid transfer free energy. Vertical reactions are experimentally accessible with chemical denaturation. Horizontal reactions are theoretically possible but not accessible by experiment. The abbreviation Aro is used to denote a Trp, Tyr, or Phe side chain.

Shown in Figure 2A,B are the transfer free energies determined for the aromatic side chains. These data indicate that all lipid-facing point mutations of the aromatic side chains either maintained ($\Delta\Delta G^{\circ}_{W,L}$ near zero) or increased (negative $\Delta\Delta G^{\circ}_{W,L}$) the folding stability of OmpLA relative to Ala mutations. Moreover, we observed an energetic gradient for Trp and Tyr in which the greatest contribution to the membrane protein stability was found for sites located in the membrane interface. For Trp it can be observed that the free energy of stabilization approaches −3.5 kcal mol^{-1} in the interfacial region; Trp sites located near the membrane center are only stabilizing by about −1 kcal mol^{-1}. Similar behavior was found for Tyr, where the stabilization energy approaches −2.5 kcal mol^{-1} in the interfacial region but is only about −0.5 kcal mol^{-1} at the membrane center. In contrast, Phe showed no

DOI: 10.1021/jacs.6b03460
J. Am. Chem. Soc. 2016, 138, 7946−7950

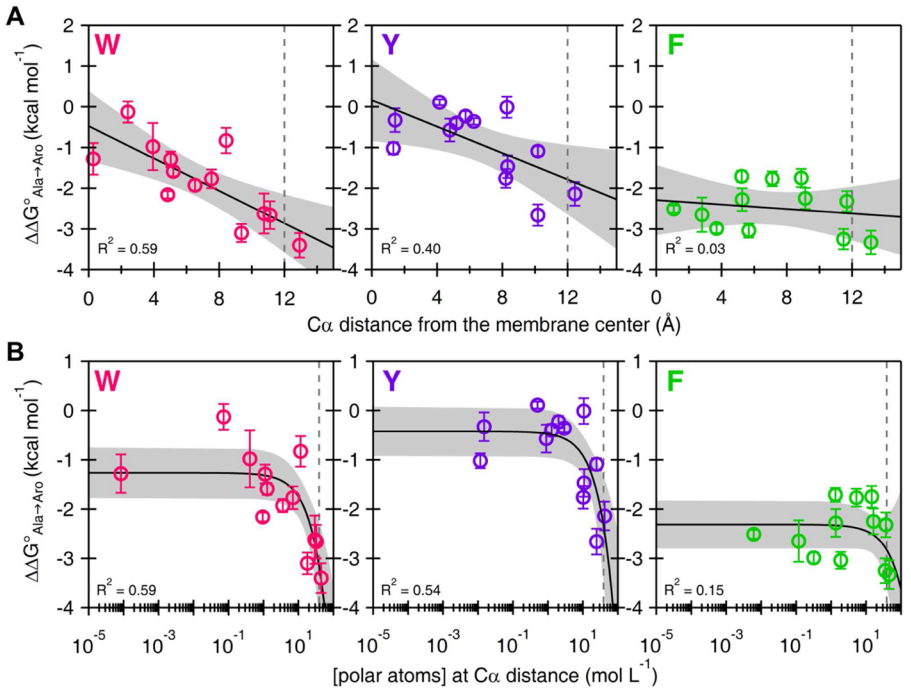

Figure 2. Aromatic side chain water-to-lipid transfer free energies show a depth dependence that is correlated with the concentration of polar atoms at the membrane positions of host sites. Side chain identities are located in the top left corners of the individual panels using one-letter codes; shown in the bottom left corners are the coefficients of determination (R^2) from linear fits. Each fit is shown in black, and the 95% confidence intervals are shown as gray-shaded regions. The beginning of the interfacial region is indicated by the dashed lines and is defined as the maximal position of the carbonyl functional groups (12 Å, occurs at [polar atoms] = 39 M). Standard errors from independent titrations ($n = 2$) are shown. (A) Transfer free energies plotted as a function of the depth of host sites. The intercepts for these fits are −0.474, 0.164, and −2.293 kcal mol^{-1} for Trp, Tyr, and Phe, respectively. The slopes are −0.199, −0.163, and −0.027 kcal mol^{-1} Å^{-1} for Trp, Tyr, and Phe, respectively. (B) Transfer free energies plotted as a function of the molar concentration of polar atoms at the depths of host sites (shown on a log scale). From the linear fits, the slopes were found to be −0.0486, −0.0491, and −0.0132 kcal L mol^{-2}, respectively, and the intercepts were determined to be −1.263, −0.423, and −2.313 kcal mol^{-1} for Trp, Tyr, and Phe, respectively.

strong depth dependence, with stabilization energies in the range of −2 to −3 kcal mol^{-1} across the entire bilayer.

Hydrophobicity is a defining force in protein folding, and water-to-nonpolar transfer free energies are intimately related to the rearrangement of water molecules. When a hydrophobic molecule (i.e., a hydrophobe) is placed in water, it is unable to participate in hydrogen bonding, which causes an ordering of water molecules around the hydrophobe. This ordering of water disrupts the hydrogen-bonding network present in liquid water. However, if this hydrophobe is transferred from water into a hydrophobic medium, there is an overall gain in entropy of the system because the bulk water gains higher configurational entropy. This increase in entropy is a large component of the free energy of this transfer (e.g., $-T\Delta S$). Because the membrane naturally possesses a changing density of polar atoms, we hypothesized that depth-dependent side chain water-to-lipid transfer energetics would reflect this physical property.

To test this idea, we sought a correlation between the transfer free energy data ($\Delta\Delta G^{\circ}_{W,L}$) and the concentration of polar atoms present at the depths of host sites. Computational Methods in the Supporting Information, Figures S4−S8, and Tables S6−S8 describe the procedure used to arrive at Figure 2B. Fits to these data indicated that the concentration of polar atoms at host sites was best correlated with our measurements (Table S9). Further inspection of the Trp and Tyr fits shows that the transfer free energies are flat in the membrane center, indicating that the hydrophobicity is constant where the concentration of polar atoms is also constant. This analysis shows that the concentration of polar atoms across the membrane normal is an important parameter in modeling water-to-lipid transfer free energies.

Aromatic−Aromatic Interactions Can Make Significant Contributions to the Cooperative Folding Energies of Membrane Proteins. In addition to the depth dependence of the energetics across the bilayer normal, we identified significant aromatic interactions with a native Tyr (residue 195) upon the introduction of either a Tyr or Trp side chain at host site 173 (Figure 3A). These pairs are located on the lipid-facing surface, and the sites are on adjacent strands, which form a cross-strand interaction. Cooperative interaction energies for YY pairs (Y195 and 173Y) or YW pairs (Y195 and 173W) were derived from double-variant cycles following the method of Serrano et al.[21] We additionally measured the interaction energy of a "flipped" WY pair (195W and 173Y). Folding data for these variants are shown in Figure S9, and folding free energies and notations of the variants are shown in Table S10. Double-variant cycles are illustrated in Figure 3A and show that the interaction energies between these pairs varied from favorable (−2.12 ± 0.19 and −0.67 ± 0.42 kcal mol^{-1} for YY and YW, respectively) to unfavorable (+0.25 ± 0.42 kcal mol^{-1} for WY).

The physical explanation for these results is complex. Interaction energies between aromatic pairs may vary because of the chemical composition, the orientation of these side chains, or other factors such as the protein or lipid environment. Despite being composed of identical side chains,

DOI: 10.1021/jacs.6b03460
J. Am. Chem. Soc. 2016, 138, 7946−7950

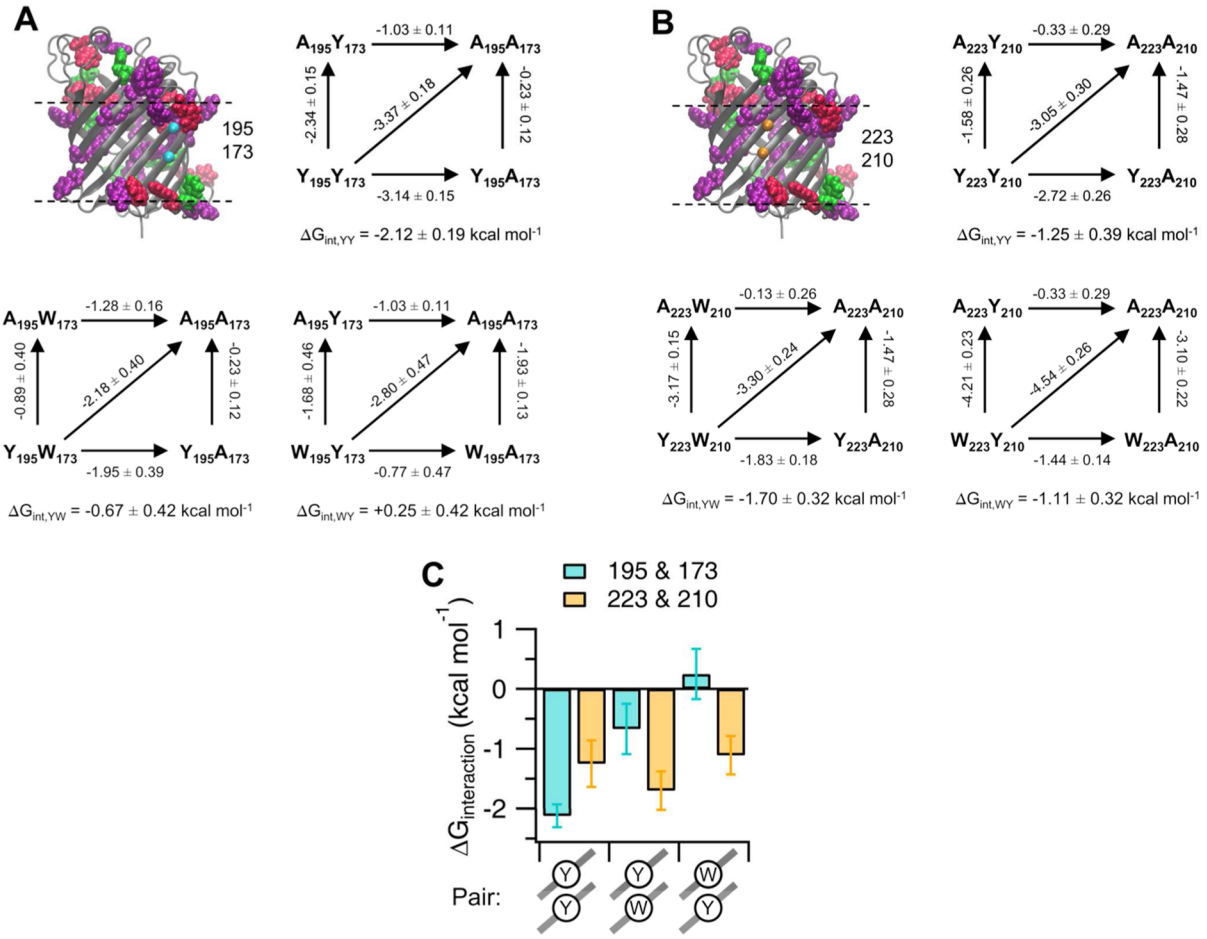

Figure 3. Coupling of aromatic pairwise interactions is influenced by an aromatic network. (A) Coupling energetics measured at sites 195 and 173. Cα atoms of host sites on the lipid-facing surface of OmpLA are shown as cyan spheres. Double-variant cycles used to determine the interaction energies between aromatic pairs are also shown. The interaction energy was calculated as previously described[21] and is shown underneath each cycle. Numbers by the arrows indicate the difference in stabilities between variants and are in units of kcal mol^{-1}. Highlighted are the aromatic side chains Trp (pink), Tyr (purple), and Phe (green) from a wild-type MD simulation, and planes of the phosphorus atoms are shown as dashed lines. (B) Same as in (A) for pairs measured at sites 223 and 210, shown as orange spheres. (C) Summary of the measured interaction energies. The cross-strand pair types are illustrated schematically below the bar graph. Standard errors from independent titrations (n = 2) are shown. Protein images were generated using VMD.[20]

the magnitudes of the interactions between YW and the flipped WY pairs were the most different from each other. Confounding a simple interpretation is the observation that the interaction magnitudes of FF or YY pairs were found to be identical (−1.3 kcal mol^{-1}) when introduced on the surface of the soluble protein barnase.[21] An additional factor for consideration is that inspection of the side chains surrounding site 195 in the crystal structure of OmpLA reveals that it is part of a larger aromatic network composed of Trp and Tyr side chains located at the membrane interface (Figure 3A).

To test whether an aromatic network could influence the pairwise energetics, we engineered these aromatic pairs at different host sites (A223 and A210) that were devoid of aromatics within the surrounding side chains and located at the same z depth in the membrane as sites 195 and 173 (Figure 3B). Double-variant cycles at these sites are shown in Figure 3B, and the folding free energies are presented in Table S10 and Figure S9. As shown in Figure 3C (gold), compared with the values at sites 195 and 173 (cyan), these experiments revealed that the interaction energies were instead favorable in all cases and within error of each other at this control location. Taken together, these data demonstrate that aromatic–aromatic interactions are influenced by the presence of aromatic networks.

DISCUSSION

Using thermodynamic cycle analysis of membrane protein folding into lipid vesicles, we measured the water-to-lipid transfer free energies of aromatic amino acid side chains as a function of depth in the bilayer. In contrast to an early study,[22] our measurements indicate a thermodynamic enhancement for Trp and Tyr at the membrane interface compared with the bilayer center. Our work shows that the depth-dependent free energy changes are well-described by the concentration of polar atoms present in the membrane polarity gradient. We rationalize that the physical basis for our results is dominated by the interactions between aromatic groups and water and is therefore modulated by the steeply changing concentration of water across the bilayer. In contrast to hydrophobicity measurements carried out in nonpolar solvents, our use of phospholipid bilayers as our hydrophobic "solvent" allows us to naturally access this steeply changing gradient in our interrogation of water-to-bilayer solvation energies. For this reason, we expect that our findings will be generally applicable to

DOI: 10.1021/jacs.6b03460
J. Am. Chem. Soc. 2016, 138, 7946−7950

bilayers composed of many lipid types and membrane thicknesses. For instance, the identity of the headgroup should not significantly affect the polar atom concentration gradient, especially near the membrane center. Similarly, the energetic gradient is relevant to membranes with greater hydrophobic thicknesses than employed here because increases in hydrophobic thickness will only enlarge the z range over which the water concentrations are essentially constant (and low) in the center of the bilayer.

In addition to aromatic placement at the membrane interface, aromatic−aromatic pairwise interactions can be significant to membrane protein stability. As observed previously,[23] the magnitudes of these coupling energies can be on the order of the transfer free energies alone. However, it is also clear that these nearest-neighbor interactions depend on the local environment, as one pair (195W/173Y) was found to show an unfavorable coupling energy that may have been influenced by nearby aromatic clusters. Further investigation of this issue is required in order to elucidate the energetic and structural details of such interactions, which can be important because such networks are enriched in thermophilic proteins[24] and line the drug pockets of many enzymes.[25]

Membrane protein structures are known to be enriched in aromatic side chains forming aromatic "belts" in protein regions located at the bilayer interface. Our energetic trends recapitulate this fundamental observation and provide strong evidence for the energetic "anchoring" that is often invoked by this structural motif. Excellent quantitative agreement with the Wimley−White interfacial scale[13] for Trp and Tyr is found (Figure S10). However, a quantitative comparison between our energetic values and previous translocon-derived,[26] statistical,[9] or computational estimates[18,27] results in a low correlation coefficient (Tables S11 and S12 and Figures S10 and S11). We rationalize this by suggesting that these various methods measure the energetics in very different ways. For example, the experimentally derived translocon data have a different reference state than utilized in the present experiments.[28] Moreover, pseudo-Boltzmann energies from statistical analyses measuring the frequency of lipid-facing amino acids[8,9] do not account for the possibility that lipid-facing residues may also be there to play a functional role. Finally, potential of mean force calculations derived from prior MD simulations depend on the accuracy of the force fields, which do not generally account for the polarizability intrinsic to aromatic side chain chemistry.[29]

In conclusion, our results bring clarity to an understanding of how the steeply changing polarity gradient of the biological lipid bilayer can modulate the energetics of membrane proteins. At the same time, the nearest-neighbor coupling energies uncover increasing complexity in the forces stabilizing them.

■ ASSOCIATED CONTENT

Supporting Information

The Supporting Information is available free of charge on the ACS Publications website at DOI: 10.1021/jacs.6b03460.

Methods and supplemental tables and figures (PDF)

■ AUTHOR INFORMATION

Corresponding Author

*Karen.Fleming@jhu.edu

Notes

The authors declare no competing financial interest.

■ ACKNOWLEDGMENTS

This work was funded by NIH Grants R01 GM079440 and T32 GM008403, and NSF grant MCB1412108. We thank Margo Goodall, Dr. Nathan Zaccai, and the QB3 macrolab for assistance in cloning the variants in this study and Dr. Patrick Fleming for guidance on the molecular dynamics simulations.

■ REFERENCES

(1) Yildirim, M. A.; Goh, K. I.; Cusick, M. E.; Barabasi, A. L.; Vidal, M. *Nat. Biotechnol.* **2007**, *25*, 1119.
(2) Dill, K. A. *Biochemistry* **1990**, *29*, 7133.
(3) Rose, G. D.; Geselowitz, A. R.; Lesser, G. J.; Lee, R. H.; Zehfus, M. H. *Science* **1985**, *229*, 834.
(4) Rees, D. C.; DeAntonio, L.; Eisenberg, D. *Science* **1989**, *245*, 510.
(5) Schiffer, M.; Chang, C.-H.; Stevens, F. *Protein Eng., Des. Sel.* **1992**, *5*, 213.
(6) Wallin, E.; Tsukihara, T.; Yoshikawa, S.; von Heijne, G.; Elofsson, A. *Protein Sci.* **1997**, *6*, 808.
(7) Ulmschneider, M. B.; Sansom, M. S.; Di Nola, A. *Proteins: Struct., Funct., Genet.* **2005**, *59*, 252.
(8) Senes, A.; Chadi, D. C.; Law, P. B.; Walters, R. F.; Nanda, V.; Degrado, W. F. *J. Mol. Biol.* **2007**, *366*, 436.
(9) Hsieh, D.; Davis, A.; Nanda, V. *Protein Sci.* **2012**, *21*, 50.
(10) Slusky, J. S.; Dunbrack, R. L., Jr. *Bioinformatics* **2013**, *29*, 2122.
(11) Killian, J. A.; von Heijne, G. *Trends Biochem. Sci.* **2000**, *25*, 429.
(12) Jacobs, R. E.; White, S. H. *Biochemistry* **1989**, *28*, 3421.
(13) Wimley, W. C.; White, S. H. *Nat. Struct. Biol.* **1996**, *3*, 842.
(14) Yau, W.-M.; Wimley, W. C.; Gawrisch, K.; White, S. H. *Biochemistry* **1998**, *37*, 14713.
(15) Wolfenden, R. *J. Gen. Physiol.* **2007**, *129*, 357.
(16) Wiener, M. C.; White, S. H. *Biophys. J.* **1992**, *61*, 434.
(17) White, S. H.; Wimley, W. C. *Biochim. Biophys. Acta, Rev. Biomembr.* **1998**, *1376*, 339.
(18) MacCallum, J. L.; Bennett, W. F.; Tieleman, D. P. *Biophys. J.* **2008**, *94*, 3393.
(19) Snijder, H. J.; Ubarretxena-Belandia, I.; Blaauw, M.; Kalk, K. H.; Verheij, H. M.; Egmond, M. R.; Dekker, N.; Dijkstra, B. W. *Nature* **1999**, *401*, 717.
(20) Humphrey, W.; Dalke, A.; Schulten, K. *J. Mol. Graphics* **1996**, *14*, 33.
(21) Serrano, L.; Bycroft, M.; Fersht, A. R. *J. Mol. Biol.* **1991**, *218*, 465.
(22) Hong, H.; Rinehart, D.; Tamm, L. K. *Biochemistry* **2013**, *52*, 4413.
(23) Hong, H.; Park, S.; Jimenez, R. H. F.; Rinehart, D.; Tamm, L. K. *J. Am. Chem. Soc.* **2007**, *129*, 8320.
(24) Kannan, N.; Vishveshwara, S. *Protein Eng., Des. Sel.* **2000**, *13*, 753.
(25) Chourasia, M.; Sastry, G. M.; Sastry, G. N. *Int. J. Biol. Macromol.* **2011**, *48*, 540.
(26) Hessa, T.; Meindl-Beinker, N. M.; Bernsel, A.; Kim, H.; Sato, Y.; Lerch-Bader, M.; Nilsson, I.; White, S. H.; von Heijne, G. *Nature* **2007**, *450*, 1026.
(27) Lin, M.; Gessmann, D.; Naveed, H.; Liang, J. *J. Am. Chem. Soc.* **2016**, *138*, 2592.
(28) Capponi, S.; Heyden, M.; Bondar, A.-N.; Tobias, D. J.; White, S. H. *Proc. Natl. Acad. Sci. U. S. A.* **2015**, *112*, 9016.
(29) Tsuzuki, S.; Uchimaru, T. *Curr. Org. Chem.* **2006**, *10*, 745.

DOI: 10.1021/jacs.6b03460
J. Am. Chem. Soc. 2016, 138, 7946−7950